



## Gated Detection Measurements of Phosphorescence Lifetimes

Yordan Kostov, Govind Rao

*Dept. of Chemical and Biochemical Engineering,*

*University of Maryland Baltimore County, 1000 Hilltop circle, Baltimore MD 21250, U.S.A.*

*E-mail: [kostov@umbc.edu](mailto:kostov@umbc.edu)*

**Abstract:** *A low-cost, gated system for measurements of phosphorescence lifetimes is presented. An extensive description of the system operating principles and metrological characteristics is given. Remarkably, the system operates without optical filtering of the LED excitation source. A description of a practical system is also given and its performance is discussed. Because the device effectively suppresses high-level background fluorescence and scattered light, it is expected to find wide-spread application in bioprocess, environmental and biomedical fields.*

**Keywords:** *Optical sensor, Gated detection, Autofluorescence, Low-cost, Filterless*

### Introduction

Phosphorescence lifetime measurements are used in many and diverse applications in analytical sensing. During the last decade, multiple reports on the detection of different analytes appeared. Most often, the method is used in the detection of oxygen concentrations, [1-5] but there are also a significant number of scientific reports concerning the detection of pH, [6-8] CO<sub>2</sub>, [9, 10] Na<sup>+</sup> and K<sup>+</sup> [11, 12] and other analytes. While the oxygen and pH directly affect the luminescence lifetime, the other are measured using complex chemistries. Many commonly used fluorescence indicators have lifetimes that are in the range of several nanoseconds or less. A sensor based on such a dye would require electronics that operate at frequencies of 10 to 100 MHz or higher. While this is achievable with the components presently used in telecommunications and computing, the sensor will be quite sophisticated and rather sensitive to interferences. For this reason, long lifetime probes that allow the use of low-cost, conventional electronics [13-15] are preferred. Another attractive feature of the long lifetime indicators is the relative ease of spectral separation; as the luminescence emission occurs from triplet state [16], the excitation and the emission maxima are usually spaced further apart than the singlet emissions. However, these attractive features are used best suited



to non-scattering, fluorescence-free samples. When a real-world sample is analyzed, the situation may become quite different.

It is well known that even small fractions of short-lived emissions or scattered light can significantly distort the lifetime measurement [17]. In order to decrease this influence, interference filters (or even monochromators) are used. However, no filter or wavelength selection device completely discards the “unwanted” light, but simply provides significant attenuation. In addition, these devices exhibit significant angular dependence on transmitted light. Consequently, there is a need for precise mechanical alignment of the optical components. These filters also need to be tightly matched with the dye; changes in the emission wavelength require changes in the filter selection. It should be also noted that the wavelength-selection devices are often the most expensive parts.

Typically, the level of the background fluorescence is significant; many naturally occurring fluorphores readily emit at the wavelengths of interest. In optical sensors, positioning of an optically opaque stratum between the sensing layer and analyte sample solves this problem. However, another difficulty arises: the optical barrier must be “transparent” to the analyte, offering minimal resistance to mass transfer. The barrier can be introduced in different ways: by dispersing a non-transparent powder in the sensing layer [18] or by creating a two-layer “sandwich” [15]. However, its presence usually results in a significant increase in the response time of the sensing layer.

Most of these problems can be solved using a different technique known as gated detection. With this method, the photodetector is turned off just long enough for the scattered light and the background fluorescence to decay to 0. This approach is feasible, because the three phenomena exist on a different time scale: the scattered light decays on the order of picoseconds, the background fluorescence has lifetime of several nanoseconds, while the phosphorescent lifetime can range from hundreds of nanoseconds up to milliseconds and seconds. The method has been extensively described [19] and optimized [20]. There are several variations of the method in both time-domain and frequency-domain fluorometry [21-23]; however, the potentially low-cost approaches have been demonstrated [24] using a storage oscilloscope and La or Tb complexes, which exhibit lifetimes in the order of milliseconds. The method is used for both intensity and lifetime measurements; however, few



described systems are useful for detecting lifetimes on micro- or nanosecond scale, and none of them are low-cost [23-25]. In this paper, we describe the principles of the operation of a novel low-cost gated system for monitoring phosphorescence lifetimes. The system is all solid state and can measure phosphorescence lifetimes longer than 200 ns. No filtering of the excitation source is employed. The system efficiently suppresses the interference from the scattered light and significant amounts of background fluorescence. It is able to operate under ambient light conditions. An extensive mathematical description and analysis is included. The real-life performance of the system is discussed.

## **Description of the gated detection system**

### **A. Design considerations and theory of operation**

Gated detection requires the use of a light source with a short switch-off time, i.e. it has to be considerably shorter than lifetime of the fluorophore under test. The energy of the light pulse must be sufficient to excite phosphorescence, with intensity that is great enough to be detected by a low cost photodetector. There are two types of pulse shapes that fulfill these requirements: delta-function and square-wave. Approximation of the first excitation type is delivered by flash lamps or pulsed lasers. However, these light sources are not low-cost, even in the case of laser diodes (short-wavelength laser diodes are still not widely available). The logical choice for the purpose of sensing is the light emitting diode (LED). Since LEDs do not have sufficient peak power to be used for delta-function excitation, a square wave pulse shape was chosen. Recently, it has been shown this can be applied to frequency domain phase fluorometry [24].

When the sample is excited with a square-wave light pulse with period  $T$ , the phosphorescence increases and decreases exponentially (Fig. 1). The light at the detector includes the fluorescence from the background and analyte, some scattered light and the analyte phosphorescence signal.

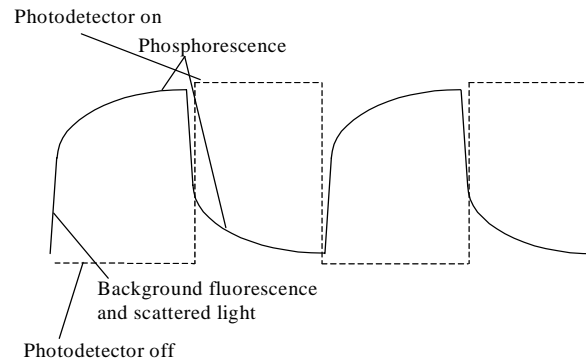


Fig. 1 Gated detection of the phosphorescence. The detector is turned on after the scattered light and the short-lived fluorescence has decayed to 0.

As the signals from fluorescence and scattered light reach steady state very quickly after the stepwise change in the excitation light, a “gate” (turning the photodetector off or disconnecting it from the signal path) for some short time  $t_g$  after the step change effectively removes the fast transients. The signal on the output of the gated amplifier is thus given by [20].

$$X(t) = \begin{cases} 0, & 0 \leq t < T/2 + t_g \\ A_m + A_B - \frac{A_m e^{-t/\tau}}{1 + e^{-T/\tau}}, & T/2 + t_g < t \leq T \end{cases} \quad (1)$$

Here,  $A_m$  is a constant that represents the initial value of the phosphorescence emission, which depends on the gate width, excitation intensity and quantum yield of the dye,  $A_B$  is the combined intensity of the scattered light and the steady-state emission of the background fluorescence,  $\tau$  is the phosphorescence lifetime,  $T$  is the period of the excitation light, and  $t_g$  is the width of the gate.

There are numerous methods for determination of the fluorophore lifetime using the resulting decay curve. The most accurate approach includes digitizing the decay curve and the use of least-squares fitting; however, this requires very-high-speed A/D converters, which are relatively expensive. In the particular case of the low-cost sensor, a hardware solution is most cost-effective. One possibility is to apply a Fourier transform by mixing the obtained signal with sine and cosine signals, averaging the results and finding the ratio of the two outputs. In this case, the output signal is given by



$$Y = \frac{\int_{T/2+t_g}^T \sin(\omega t) \cdot X(t) \cdot dt}{\int_{T/2+t_g}^T \cos(\omega t) \cdot X(t) \cdot dt} \quad (2)$$

where  $\omega = 1/(0.5T - t_g)$ .

After solving the integrals and rearranging, the following equation for the lifetime  $t$  is found:

$$\tau = \frac{Y}{\omega} \quad (3)$$

The approach is well established for use in lock-in amplifiers and it has the advantage that the output is linear with  $\tau$ . In order to suppress the ambient and scattered light, the period of the harmonic signals should be exactly  $T_m = T/2 - t_g$ . However, a highly stable, low distortion sine-wave generator is rarely low-cost. In practice, the sensor should be equipped with a frequency synthesizer to create the required signal shape with accurate timing. Furthermore, the fast sine wave mixers are a source of significant distortions and temperature instabilities.

A low-cost alternative is the use of square-wave generators and mixing. Quartz-stabilized square wave clocks are widely used and very low-cost. As mixers, simple semiconductor switches are used. Additionally, the signal-level compatibility and the simplicity of the interfacing make them very attractive for use in low-cost systems.

In the case of square-wave mixing (Fig. 2) the signal  $X(t)$  is multiplied by  $Z_1(t)$  and  $Z_2(t)$ , where

$$Y = \frac{\int_{T/2+t_g}^T Z_1(t) \cdot X(t) \cdot dt}{\int_{T/2+t_g}^T Z_2(t) \cdot X(t) \cdot dt} \quad (4)$$

$$Z_1(t) = \begin{cases} 1, & T/2 + t_g \leq t < T_m/4 \\ -1, & T_m/4 \leq t < 3T_m/4 \\ 1, & 3T_m/4 \leq t < T_m \end{cases}, \quad Z_2(t) = \begin{cases} 1, & T/2 + t_g \leq t < T_m/2 \\ -1, & T_m/2 \leq t < T_m \end{cases} \quad (5)$$

In this case, the ratio of the two integrals is no longer linear with respect to  $\tau$  yielding:



$$Y = \frac{1 - e^{-\frac{T_m}{4\tau}}}{1 + e^{-\frac{T_m}{4\tau}}} \quad (6)$$

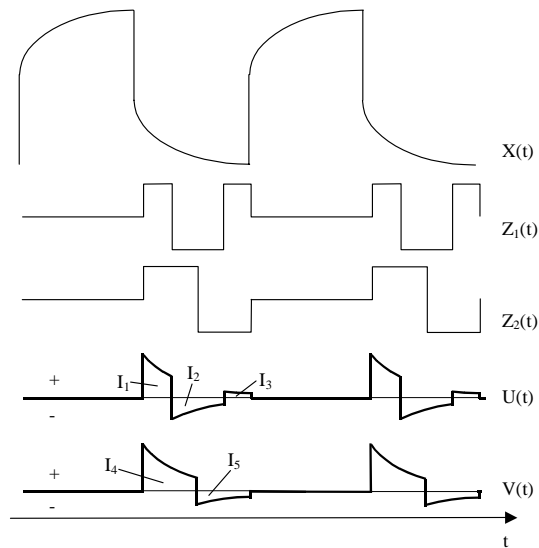


Fig. 2 Input signal X(t) and square-wave mixing signals Z<sub>1</sub>(t) and Z<sub>2</sub>(t).  
U(t) and V(t) present the signal shape before the integration.

Again, as in the case with the Fourier transforms, the signals from the ambient and scattered light are rejected. As the result is obtained in closed form, it is possible to directly calculate the lifetime of the fluorophore, if the value of ratio is known:

$$\tau = \frac{T_m}{4 \ln \left( \frac{1-Y}{1+Y} \right)} \quad (7)$$

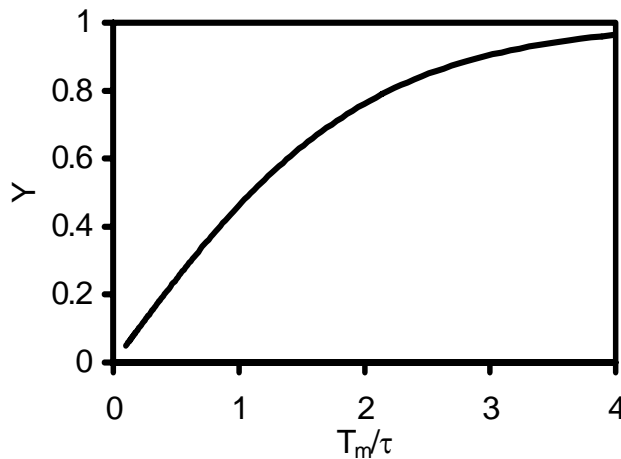


Fig. 3 Transfer function of the system



The graph of the transfer function  $Y\left(\frac{T_m}{\tau}\right)$  is shown on Fig. 3.

The resulting function is similar to the results of the rapid lifetime determination (RLD) method [25, 26]. However, our approach relies on the integration during 4 time intervals, which allows the use of binary counters and simplifies the timing logic.

### B. Metrological analysis

The system is to be used for monitoring the lifetimes of phosphorescent dyes that are used as chemical indicators. Their variation depends on the properties of the dye, which are usually well known. For example, in oxygen sensing the lifetime of  $\text{Ru}(\text{diphenyl phenanthroline})_3^{2+}$  varies approximately 3 times when the  $\text{O}_2$  concentration changes from 0% to 20.9% [27]; the dyes used for oxygen sensing typically have ratios  $\tau_{\max}/\tau_{\min}$  ( $\tau_{\max}$  is the lifetime in absence of oxygen and  $\tau_{\min}$  is the lifetime in air) in the range 2 to 5. Knowing the extent to which the lifetime of the dye varies, it is possible to optimize the dynamic range of the sensing system. It is accomplished through proper selection of the ratio  $T_m/\tau_{\max}$ . The dependence of the range on the ratio  $T_m/\tau_{\max}$  at different values of  $\tau_{\max}/\tau_{\min}$  is presented on Fig. 4. There is a well-defined maximum, which indicates that the largest dynamic range is achieved when the ratio  $T_m/\tau_{\max}$  is between 2 and 3. This value can be fine tuned knowing the exact values of the lifetimes at both ends of the range.

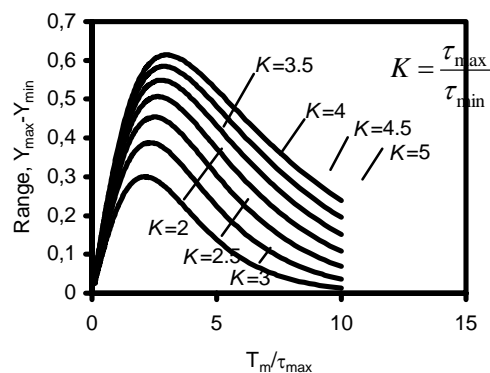


Fig. 4 Dependence of the range on the ratio between the integration window and maximum lifetime of the fluorophore.

The dependencies are given for different values of the ratio  $\tau_{\max}/\tau_{\min}$ .



The sensitivity  $S$  of the device is given by the equation

$$S = \frac{dY}{d(T_m/\tau)} = \frac{2e^{-\frac{T_m}{\tau}}}{\left(1 + e^{-\frac{T_m}{\tau}}\right)^2} \quad (6)$$

It is highest when  $T_m/\tau$  approaches 0. In practice, the sensitivity is the highest when  $T_m/\tau$  is lowest, i.e. when the lifetime of the fluorophore is the longest.

An important issue is the error of the system. As its transfer function is available in closed form, it is possible to use a standard error propagation technique [28] to evaluate the uncertainty of the decay time determination. This yields

$$\sigma_\tau = \frac{-0.5T_m}{\ln^2\left(\frac{1-Y}{1+Y}\right)} \frac{Y}{1-Y^2} \left( \frac{\sigma_{I_1}^2 + \sigma_{I_2}^2 + \sigma_{I_3}^2}{(I_1 - I_2 + I_3)^2} + \frac{\sigma_{I_4}^2 + \sigma_{I_5}^2}{(I_4 - I_5)^2} \right)^{\frac{1}{2}} \quad (7)$$

where  $I_1, I_2, I_3, I_4$  and  $I_5$  are the respective integrals of the decay curve (Fig. 2).  $\sigma_{I_1} - \sigma_{I_5}$  were considered to be result of the Poisson noise, i.e.  $\sigma_{I_n} = I_n^{1/2}$  over the entire decay curve. Values

for the integrals were generated using  $I_0 \tau e^{-\frac{t_1}{\tau}}$  (fluorescence intensity at the moment when the gate is turned on) equal to 10000 and an integration window that varies between 0.2 and 5. For comparison, the error curve of the original RLD method for the same conditions (presence of ambient light) was calculated.

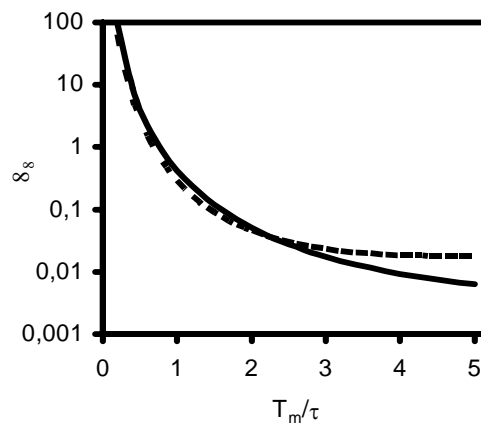


Fig. 5 Comparison between error of the proposed detection method and the standard rapid lifetime determination. Solid line - the uncertainty of the proposed method, dashed line - the uncertainty of the RLD



As can be seen in Fig. 5, the error rapidly decreases with an increase of the length of the integration window. At smaller ratios  $T_m/\tau$  ( $< 2.3$ ), the uncertainty of the classic RLD with baseline determination [26] is smaller; however, above that value the error of our system is smaller.

### C. Description of the practical system

The schematic representation of the system is given in Fig. 6. A cuvette with solution of a long-lifetime fluorophore was positioned in front of a PIN photodiode (S7329 Hamamatsu, Japan). The excitation source, a blue LED NSPB 500 (Nichia, Japan), was oriented at  $45^\circ$  to the cuvette front wall, while the photodetector was oriented parallel to it. In this way, the majority of the reflected light did not shine directly on the photodetector. The LED is driven by a fast driver (ECL type [29]), which provides short rise and fall times of 10 and 12 ns, respectively. The light from the LED was not filtered at all. In front of the light receiver, a low-cost red plastic filter (Colored CR-39, light red, Fosta-Tek, Leominster, MA) was placed. The absorbance of the filter is approximately 1.8 in the stop band and about 0.4 in the pass band, and its sole purpose was to protect the photoreceiver from saturation by removing some of the scattered LED light.

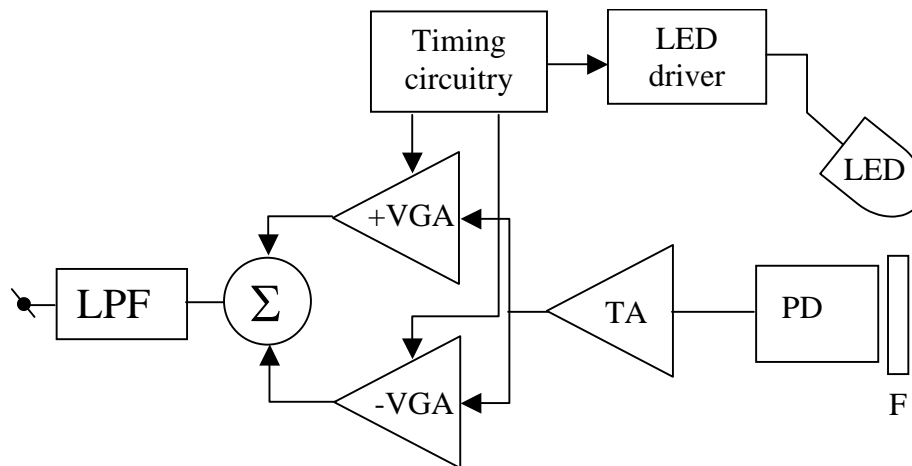


Fig. 6 Block schematic of the proposed gated detection system.

LED – light emitting diode, F – filter, PD – photodiode, TA – transimpedance amplifier,

VGA – variable-gain amplifier,  $\Sigma$  – summator, LPF – low-pass filter.

The photodetector (photodiode and transimpedance amplifier) and the subsequent amplification stages have bandwidths of 40 MHz. This prevents nonlinear distortions for signals with lifetimes down to 200 ns.



As gating stages, variable gain amplifiers (VGA) CLC5523 (National Semiconductor, Santa Clara, CA) were used. Their gain control rate is 4 dB/ns, which allows switching between 0 dB and -60 dB amplification in 15 ns. Again, as the “gate” on and off times are significantly shorter than the measured lifetimes, they do not introduce any measurable distortion in the measured phosphorescence signals.

The multiplication by 1 or -1 was performed by switching on the respective VGA (Fig. 6). The gate was introduced by decreasing the amplification of the VGA to its lowest setting (-60 dB). The timing circuitry was built on 74F family logic integrated circuits, which have typical rise and fall times of approximately 3 ns. The length of the interval was set by a programmable 8-bit counter, while the length of the gate was set by a programmable 4-bit counter. The integration intervals were timed by an additional 4-bit counter, whose outputs of the last 2 most significant bits were used to create the requested 4 equal time intervals  $t_1 \div t_4$ . The “high” and “low” output levels of the logic integrated circuits vary: between 0 and 0.8 V for the “low” state and between 3.8 and 5 V for the high state. The used VGA has relatively narrow control voltage – below 0.4 V it is completely off (-60dB) while above 1.6 V it is completely on (0dB). Using resistor attenuator, the output levels of the logic integrated circuit were divided by 2. In this way, the variation of the logic levels does not change the amplification of the amplifier and the maximum input control voltage of 2.5 V for CLC5523 is not exceeded.

The outputs from the VGA were fed into a difference amplifier built on AD 8001 (Analog Devices, Norwood, MA). Its subsequent output was averaged with a first-order lowpass filter with a time constant of 0.1 s. The output from the filter was connected to an ADC computer card, and the signal was digitized and the ratios determined numerically.

### Performance and discussion

The system was tested with three different long-lifetime dyes – *tris*(bipyridine) ruthenium dichloride, *tris*(diphenylphenanthroline) ruthenium dichloride from GFS Chemicals (Powel, OH) and platinum octaethylporphyrin (PtOEP) from Porphyrin products (Logan, UT). The first two dyes are water-soluble and were used in aqueous solutions, while the third is not and was used in DMSO solutions. The concentration of the dyes was 20  $\mu$ M. Prior to performing the tests with the system, the lifetimes of the dyes were measured with a frequency-domain



fluorometer (ISS Koala, ISS, Urbana-Champaign, IL). In all cases, an NSPB500 blue LED was used as the excitation source [30]. The lifetimes of the dyes in the respective solutions saturated with air or nitrogen are shown in Table 1. The integration windows were selected as 2.3 times the lifetime of the dye in N<sub>2</sub> in order to obtain the widest possible range (as follows from Fig. 4).

Table 1 Properties of the long-lifetime dyes, used in the system validation.

Dye	(Ru(bpy) <sub>3</sub> Cl <sub>2</sub> /H <sub>2</sub> O	Ru(dpp) <sub>3</sub> Cl <sub>2</sub> /H <sub>2</sub> O	PtOEP/DMSO
Lifetime in N <sub>2</sub>	0.54 μs	3.1 μs	53.5 μs
Lifetime in air	0.36 μs	0.7 μs	0.68 μs
Integration window	1.3 μs	7 μs	130 μs

The performance of the system was evaluated by measuring the dyes under two conditions: solution of pure dye and solution of dye in presence of an interfering short-lifetime fluorophore. For this purpose, Rhodamine B was selected (lifetime 1.4 ns), and its concentration was adjusted so that its emission intensity was 15% of the emission of the other dyes. When measured on the standard lifetime fluorometer, the addition of Rhodamine B changed the apparent lifetime (as measured in frequency domain at single frequency) of more than 200 %.

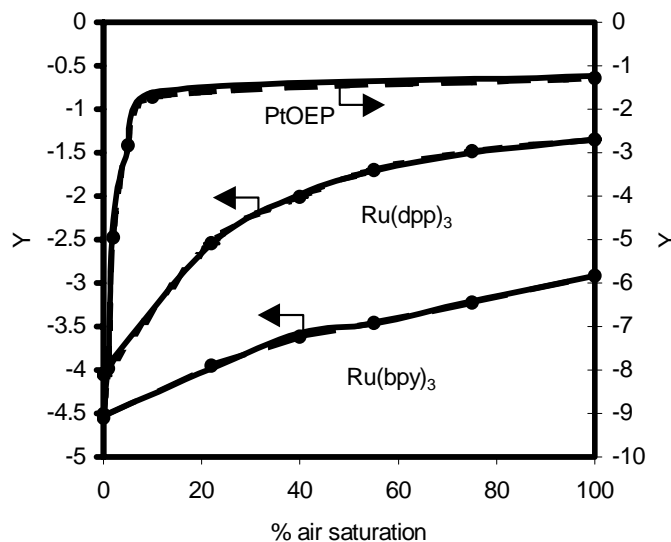


Fig. 7 Comparison between the measured output Y of the system in presence (solid line) and in absence (dashed line) of short-lived interference.



The results of the measurements of the solutions with and without interference are shown on Fig. 7. The gate width was selected to be 150 ns. The solutions were bubbled with gas mixtures with different O<sub>2</sub> concentrations. Because of the significant sensitivity of PtOEP to oxygen it was measured in the range 1-10% O<sub>2</sub> (of air saturation), while the other two dyes were measured in the range 0-100%. As can be seen in this plot, the system effectively discards the short-lived interference. There is less than 1% difference between the measurements with and without short-lived dye. The slight variations that are observed at concentrations different from N<sub>2</sub> and air are attributable to inaccuracies of the gas metering. Another possible source of error is the temperature dependence of the dyes' lifetime, which is approximately 2-3%/°C. The experiments were performed in an air-conditioned room, in which the air temperature may vary up to ±1.5°C. It should be also noted that the significant amount of scattered excitation light as well as the room light did not affect the performance of the system.

In conclusion, our system allows for the measurement of phosphorescence lifetimes in the presence of significant amounts of short-lived fluorescence and scattered light. The cost of the system is extremely low: the cost of the components is less than \$50. An obvious application of the system is for oxygen measurements in bioprocesses, where the growth media often displays strong autofluorescence. Using the system, the chemical sensors could be produced without the protective white "shield" which would result in shorter response times and lower production costs. One less obvious benefit is the elimination of the narrow band-pass filtering. As a result, the emission filter can be integrated with the photodetector. In fact, there are already some photodiodes available that are housed in colored plastic [31]. Aside from further lowering the cost (the optical components are usually the most expensive parts in an optical sensor), this also opens the possibility for production of an "all-electronics-and-chemistry-only" sensor, with simplicity that is comparable to electrochemical sensors, but without the need for direct physical contact of the transducer with the sensing phase.

### **Acknowledgements**

*This work was supported by the NSF Grant BES 0091705 and unrestricted funding from Du Pont, Fluorometrix, Genentech, Merck, and Pfizer.*



## References

1. Wolfbeis O. S. (1991). *Fiber Optic Chemical Sensor and Biosensors*, Vol. 1. Boca Raton, FL: CRC Press.
2. Lakowicz J. R. (1994). *Topics in Fluorescence Spectroscopy, Volume 4: Probe Design and Chemical Sensing*. New York, Plenum Press.
3. Kneas K., JN. Demas, B. Nguyen, A. Lockhart, W. Xu (2002). DeGraff BA, *Anal.Chem.*, V. 74, pp. 1111-1118.
4. MacGraith B. D., C. M. McDonagh, G. O'Keefe, E. T. Keyes, J. G. Vos, B. O'Kelly, J. F. McGilp (1993). *Analyst*, V. 118, pp. 385-388.
5. Bambot S. B., R. Holavanahali, J. R. Lakowicz, G. M. Carter, G. Rao (1994). *Biotech. & Bioengr.*, V. 43, pp. 1139-1145.
6. Kosch U., I. Klimant, O. S. Wolfbeis, J. Fresenius (1999). *Anal. Chem*, V. 362, pp. 48-53.
7. Clarke Y., W. Xu, J. N. Demas, B. A. DeGraff (2000). *Anal. Chem.*, V. 72, pp. 3468-3475.
8. Malins C., HG. Glever, TE. Keyes, JG. Vos, WJ. Dressick, BD. MacCraith (2000). *Sens. Actuators B*, **67**, pp. 89-95.
9. Neurauder G., I. Klimant, O. S. Wolfbeis (1999). *Anal. Chim. Acta*, V. 382.
10. von Bultzingslowen C., AK. McEvoy, C. McDonagh, BD. MacCraith, I. Klimant, C. Krause, OS. Wolfbeis (2002). *Analyst*, V. 127, pp. 1478-1483.
11. Krause C., T. Werner, C. Huber, OS. Wolfbeis, MJP. Leiner, (1999). *Anal.Chem.*, V. 71, pp. 1544-1548.
12. Z. Gryczynski, Gryczynski I, Lakowicz JR (2003). *Methods Enzymol.*, V. 360, pp. 44-75,
13. Kostov Y., A. Comte, T. Scheper (1998). *Biotechnology & Bioengineering Quarterly*, V. 12, pp. 201-205.
14. Kostov Y. H., R. S. Pilato, G. Rao (2000). *Analyst*, V. 125, pp. 1175-1178.
15. Tolosa L., Y. Kostov, P. Harms, G. Rao (2002). *Biotechnol. Bioeng.*, V. 80, pp. 594-597.
16. Demas J., BA DeGraff, PB Coleman (1999). *Anal.Chem.*, V. 71, pp. 793A-800A.
17. Lakowicz J. R. (1999). *Principles of Fluorescence Spectroscopy*. New York: Plenum Press.
18. Klimant I., OS Wolfbeis (1995). *Anal.Chem.*, V. 67, pp. 3160-3166.



19. Voigtman E., J. D. Winefordner (1986). *Anal. Instr.*, V. 15, pp. 309-328.
20. Barnes C. G., J. D. Winefordner (1984). *Appl. Spec.*, V. 38, pp. 214-228.
21. Barisas B., MD Leutner (1980). *Rev.Sci.Instr.*, V. 51, pp. 71-74.
22. Henselman D., R. Withnell, GM Hieftje (1991). *Appl. Spec.*, V. 45, pp. 1553-1560.
23. Lakowicz J., I. Gryczynski, Z. Gryczynski, ML. Johnson (2000). *Anal Biochem.*, V. 277, pp. 74-85.
24. Rowe H., SP Chan, JN Demas, BA. DeGraff (2002). *Anal. Chem.*, V. 74, pp. 4831-4827.
25. Woods R., S. Scypinski, LJ Cline Love, HA Ashworth (1984). *Anal.Chem.*, V. 56, pp. 1395-1400.
26. Ballew R., JN Demas (1989). *Anal. Chem.*, V. 61, pp. 30-33.
27. Mills A., M. Thomas (1997). *Analyst*, V. 122, pp. 63-68.
28. Bevington P. (1969). *Data reduction and error analysis for the physical sciences*. New York: McGraw-Hill.
29. Shumate P. W., Jr., DiDomenico (1982). *Lightwave Transmitters*, In: *Semiconductor devices for optical communication*, H. Kressel, Ed. Berlin: Springer Verlag, , pp. 173-176.
30. Sipior J., GM Carter, JR Lakowicz, G. Rao (1996). *Rev. Sci. Instr.*, V. 67, pp. 3795-3798.
31. Catalog H. (2002) Si photodiodes, pp. 4.